

Amplified warming of extreme temperatures over tropical land

Supplementary information

Michael P. Byrne

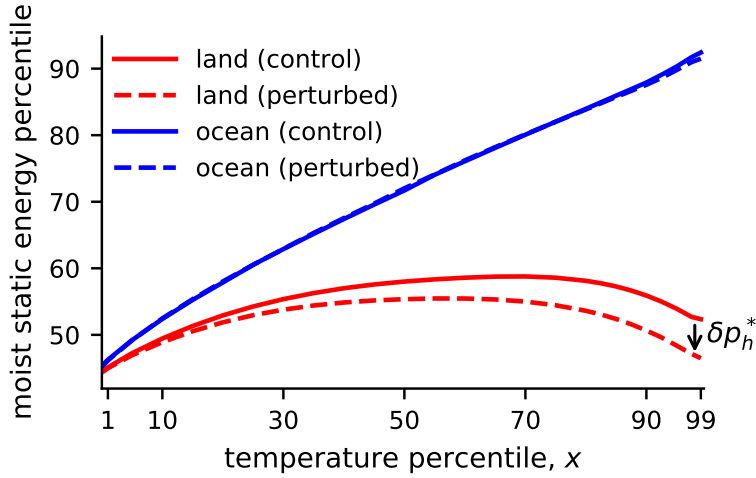


Figure S1: Moist static energy percentiles (y -axis) corresponding to the average moist static energy of days exceeding the given temperature percentile on the x -axis over land (red) and ocean (blue). Solid and dashed lines denote the control and perturbed simulations, respectively. The decrease with warming of the moist static energy percentile to which hot land days corresponds is indicated (δp_h^*).

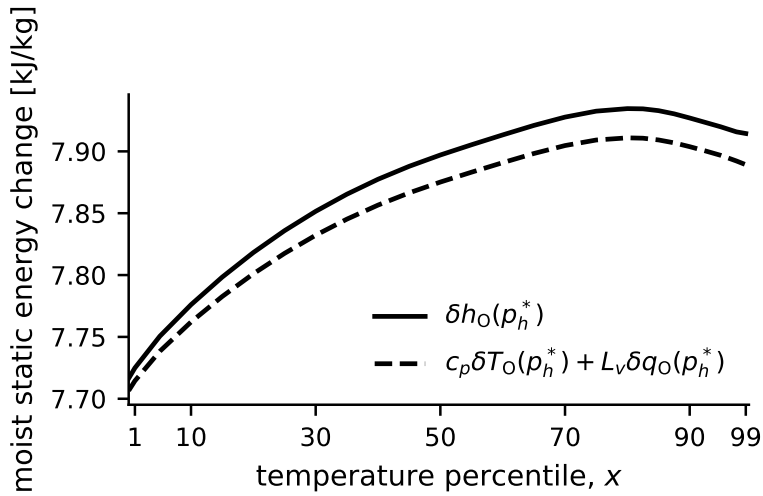


Figure S2: Change in the p_h^* -th percentile of ocean moist static energy (solid) and an estimate of this change using the p_h^* -th percentiles of ocean temperature and specific humidity (dashed). The fractional differences between the solid and dashed lines are less than 0.5% for all percentiles.

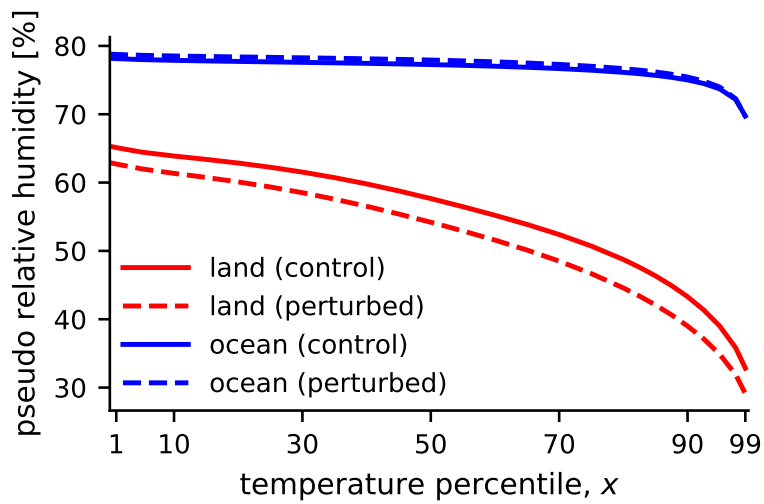


Figure S3: Pseudo relative humidity over land (red) and ocean (blue) for the control (solid) and perturbed simulations (dashed). Over land, pseudo relative humidity is defined as the average specific humidity for the hottest $(100 - x)\%$ of days divided by the corresponding average saturation specific humidity (Methods). Over ocean, pseudo relative humidity is defined as the p_h^* -th percentile of specific humidity divided by the p_h^* -th percentile of saturation specific humidity. Note that p_h^* is the percentile of land moist static energy in the control simulation equal to the average moist static energy of the hottest $(100 - x)\%$ of land days.

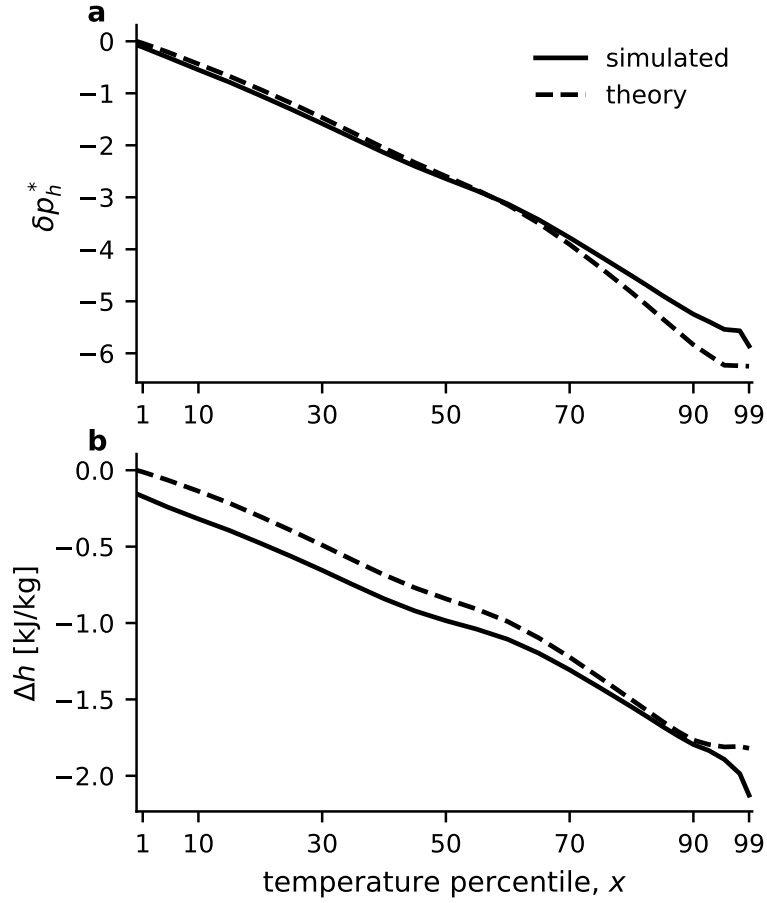


Figure S4: Simulated (solid) and theory estimates (dashed) of (a) changes in the percentile of land moist static energy equal to the average moist static energy of the hottest $(100 - x)\%$ of land days (i.e. δp_h^*) and (b) $\Delta h = h_L^{pert}(p_h^* + \delta p_h^*) - h_L^{pert}(p_h^*)$. The theory estimates in panels (a) and (b) are computed using equations (21) and (3), respectively.

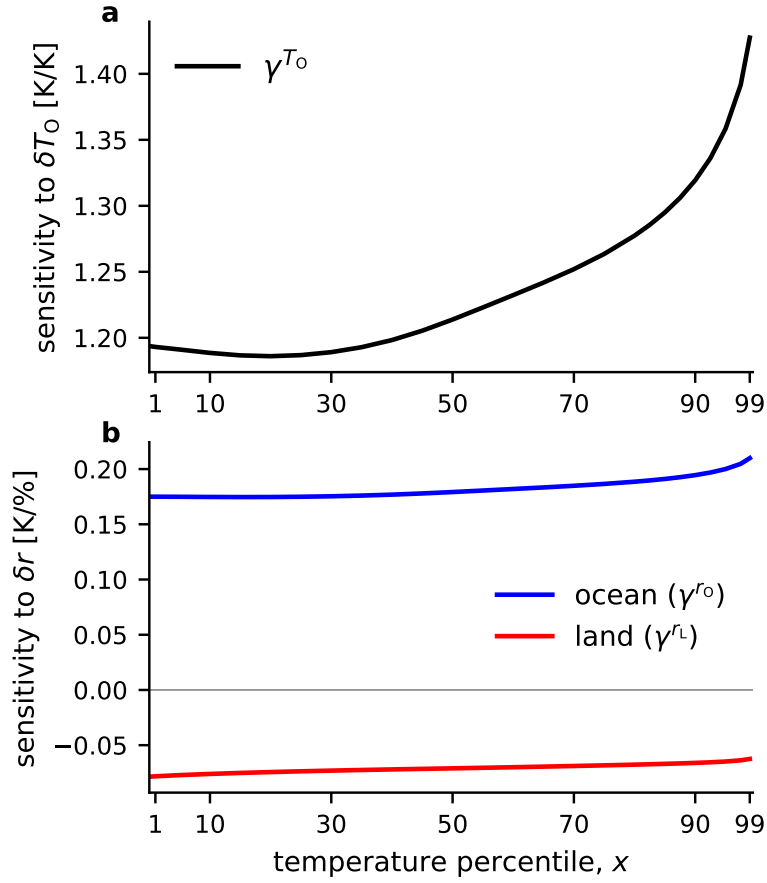


Figure S5: Parameters quantifying the sensitivities of land temperature to changes in (a) ocean temperature and (b) ocean (blue) and land relative humidities (red). The sensitivity parameters γ^{T_o} , γ^{r_o} and γ^{r_L} are defined by equations (13), (14) and (25), respectively.

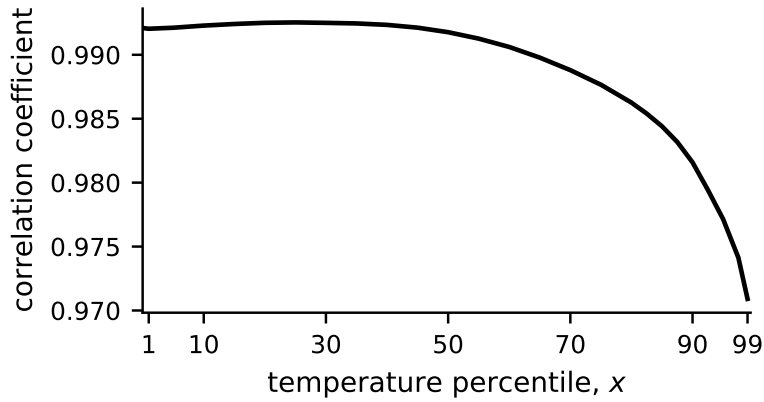


Figure S6: Correlation coefficients between simulated and estimated changes [using (4)] in average temperature for the hottest $(100 - x)\%$ of land days across climate models.

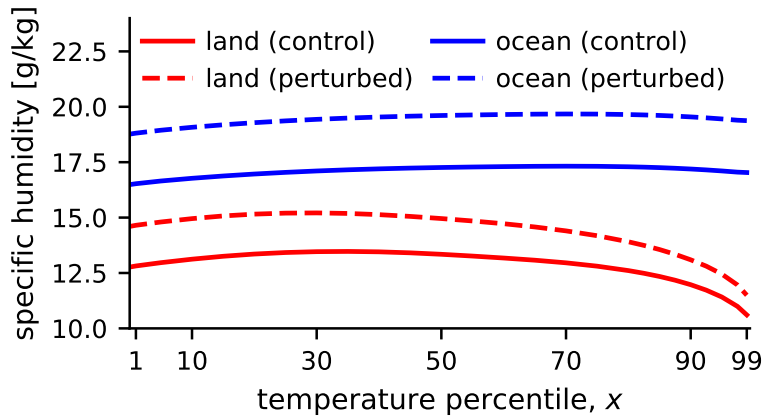


Figure S7: Specific humidity over land (red) and ocean (blue) for the control (solid) and perturbed simulations (dashed). Over land, the average specific humidities for the hottest $(100 - x)\%$ of days are shown. Over ocean, the p_h^* -th percentile of specific humidity in each simulation is plotted.

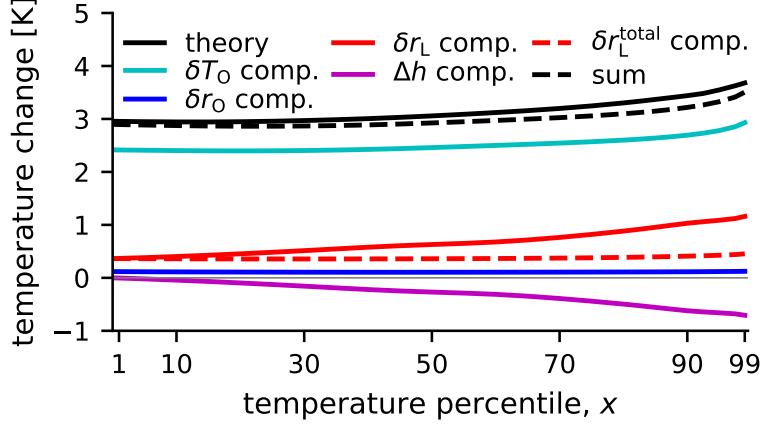


Figure S8: Theory estimate of the land temperature change [solid black, see (4)] and the four contributions to the theory (23) due to changes in ocean temperature (cyan), ocean relative humidity (blue), land relative humidity (solid red) and Δh (magenta). The sum of the four contributions (dashed black) is approximately equal to the full theory. The combined effect of changes in land relative humidity and Δh [see (24)] is indicated by the dashed red line.

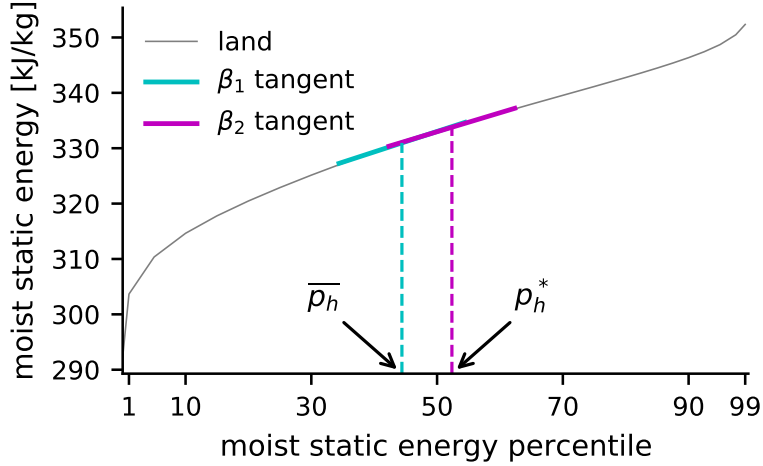


Figure S9: Land moist static energy in the control simulation vs moist static energy percentile (gray). The parameters β_1 (cyan) and β_2 (magenta) are the slopes of the tangents to $h_L(p_h)$ at \bar{p}_h and p_h^* , respectively.